

The Antibiotic CJ-15,801 Is an Antimetabolite that Hijacks and Then Inhibits CoA Biosynthesis

Renier van der Westhuyzen,^{1,5} Justin C. Hammons,^{3,5} Jordan L. Meier,³ Samira Dahesh,⁴ Wessel J.A. Moolman,¹ Stephen C. Pelly,² Victor Nizet,⁴ Michael D. Burkart,^{3,*} and Erick Strauss^{1,*}

¹Department of Biochemistry

²Department of Chemistry and Polymer Science

Stellenbosch University, Stellenbosch 7600, South Africa

³Department of Chemistry and Biochemistry

⁴Division of Pharmacology and Drug Discovery, Department of Pediatrics, and Skaggs School of Pharmacy and Pharmaceutical Sciences University of California San Diego, La Jolla, CA 92093, USA

⁵These authors contributed equally to this work

*Correspondence: mburkart@ucsd.edu (M.D.B.), estrauss@sun.ac.za (E.S.)

DOI 10.1016/j.chembiol.2012.03.013

SUMMARY

The natural product CJ-15,801 is an inhibitor of *Staphylococcus aureus*, but not other bacteria. Its close structural resemblance to pantothenic acid, the vitamin precursor of coenzyme A (CoA), and its Michael acceptor moiety suggest that it irreversibly inhibits an enzyme involved in CoA biosynthesis or utilization. However, its mode of action and the basis for its specificity have not been elucidated to date. We demonstrate that CJ-15,801 is transformed by the uniquely selective *S. aureus* pantothenate kinase, the first CoA biosynthetic enzyme, into a substrate for the next enzyme, phosphopantothenoylcysteine synthetase, which is inhibited through formation of a tight-binding structural mimic of its native reaction intermediate. These findings reveal CJ-15,801 as a vitamin biosynthetic pathway antimetabolite with a mechanism similar to that of the sulfonamide antibiotics and highlight CoA biosynthesis as a viable antimicrobial drug target.

INTRODUCTION

The antibiotic CJ-15,801 (**1**; Figure 1A) was discovered in 2001 by a Pfizer research team when it was isolated from fermenting cultures of a *Seimatosporium* sp. fungus (Sugie et al., 2001). Structural analysis showed the compound to resemble pantothenic acid (vitamin B₅, **2**; Figure 1B), the natural precursor of the essential metabolic cofactor coenzyme A (CoA, **3**) (Strauss, 2010), with the notable exception of a *trans*-substituted double bond in the β -alanine moiety. This feature imparts an *N*-acyl vinyllogous carbamic acid functionality to **1**, an uncommon motif that is also present in the anticancer agent palytoxin and lipopeptide antibiotics such as enamidonin (Han et al., 2004; Nicolaou and Mathison, 2005). Subsequently, CJ-15,801 was shown to inhibit the growth of drug-resistant strains of *Staphylococcus aureus* (MRSA) with minimum inhibitory concentration (MIC) values ranging between 6.25 and 50 μ g/ml (30–230 μ M). Interestingly, other bacteria, including *Escherichia coli*, *Haemo-*

philus influenzae, and several *Streptococcus* species, were not inhibited. In a later study, Saliba and Kirk determined that CJ-15,801 also inhibits the intraerythrocytic growth stage of the malaria parasite *Plasmodium falciparum* with an IC₅₀ value of 39 μ M, while leaving rat hepatoma tissue culture (HTC) cells unaffected (Saliba and Kirk, 2005). Moreover, the malarial inhibition was reversed when the concentration of pantothenic acid in the medium was increased. Taken together, these findings all pointed to CJ-15,801 targeting CoA biosynthesis, or an enzyme or process dependent on this cofactor (Spry et al., 2008, 2010). However, such a proposal has not been confirmed experimentally in any of the organisms sensitive to CJ-15,801, nor does it provide a satisfactory explanation for this antibiotic's peculiar selectivity.

The presence of the *N*-acyl vinyllogous carbamic acid functionality in CJ-15,801, combined with a knowledge of the chemical and biological reactivity of other inhibitors with similar reactive moieties, suggests that **1** most probably acts as an irreversible inhibitor of its biological target. Two mechanisms for such inhibition can be proposed: first, the α,β -unsaturated carbonyl moiety can act as a Michael-acceptor that would trap an active site nucleophile (Figure 1C); such a mechanism of action is seen in the structurally related daptamide family of antibiotics (Hollenhorst et al., 2011; Kucharczyk et al., 1990) and has also been exploited in the development of irreversible inhibitors of CoA disulfide reductase (van der Westhuyzen and Strauss, 2010). Second, if the carboxylate of CJ-15,801 were functionalized in an enzymatic transformation with an appropriate leaving group, this may provide sufficient activation for the formation of a reactive ketene intermediate that could similarly act as an electrophilic trap (Figure 1D). Importantly, both of these mechanisms would remain equally viable if the 4'-OH group of CJ-15,801 is phosphorylated or otherwise functionalized, suggesting it could be transformed by the CoA biosynthetic enzymes into an inhibitory CoA analog with a target downstream of the pathway. Such a mechanism of action has been demonstrated for the pantothenamides, a class of pantothenic acid analogs in which its carboxylate has been functionalized by amidation (Clifton et al., 1970; van Wyk and Strauss, 2008). For example, *N*-pentylpantothenamide (*N*5-Pan, **4**), which acts as a bacteriostatic agent in both *E. coli* and *S. aureus* (Choudhry et al., 2003), is transformed by three of the five CoA biosynthetic

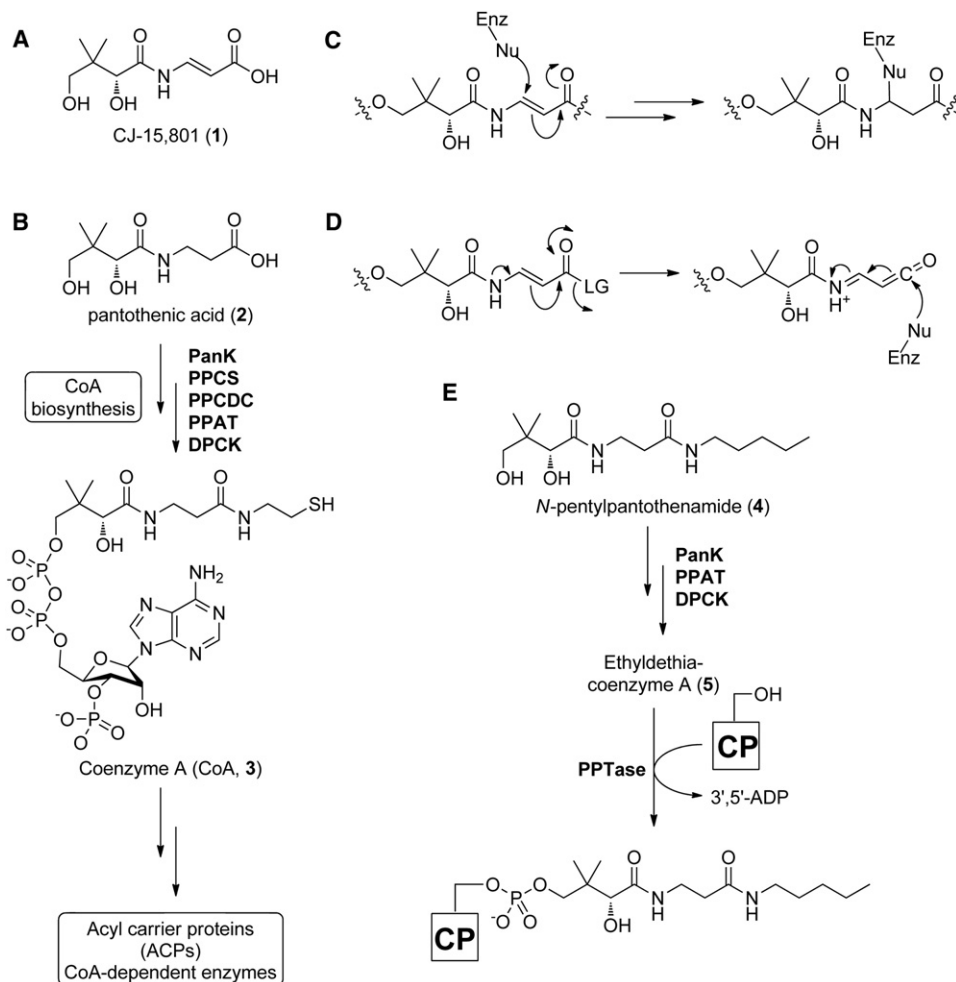


Figure 1. Structures of the Antibiotic CJ-15,801 (1), Selected Coenzyme A Biosynthetic Intermediates, Antimetabolites, and Intermediate Mimics

(A) Structure of the CJ-15,801 (1).

(B) Biosynthesis of CoA (3) from pantothenic acid (2). PanK, pantothenate kinase; PPCS, phosphopantothenoylcysteine synthetase; PPCDC, phosphopantothenoylcysteine decarboxylase; PPAT, phosphopantetheine adenylyltransferase; DPCPK, dephospho-coenzyme A kinase.

(C) Proposed mechanism for irreversible inhibition by CJ-15,801 acting as an electrophilic trap.

(D) Proposed mechanism for irreversible inhibition by CJ-15,801 after its transformation into a ketene intermediate.

(E) Biotransformation of the pantothenic acid analog *N*-pentylpantothenamide (4) to the CoA antimetabolite ethyldethia-CoA (5), which has the catalytically essential thiol of the cofactor replaced by a propyl group. The antimetabolite subsequently serves as donor in the phosphopantetheinyl transferase (PPTase)-catalyzed posttranslational modification of acyl and peptidyl carrier proteins (CPs), which results in similarly inactive *crypto*-CPs.

enzymes into ethyldethia-CoA (5), a CoA antimetabolite that lacks the thiol required for the cofactor's acyl carrier functions (Figure 1E) (Strauss and Begley, 2002). This analog subsequently serves as donor in the posttranslational modification of the *apo*-acyl carrier protein (ACP), leading to the formation of catalytically inactive *crypto*-ACP (Leonardi et al., 2005; Mercer and Burkart, 2007; Zhang et al., 2004). The resulting loss of function and subsequent impact on fatty acid metabolism is believed to be the major cause for bacteriostasis, although a recent study pointed to an impact on CoA biosynthesis as well (Thomas and Cronan, 2010).

Interestingly, like CJ-15,801, the pantothenamides also exhibit organism-based specificity. While the basis for this specificity may partially reflect differences in the targeted organism's cell

permeability and/or the nature of potential drug efflux pumps, the most important factor relates to the nature of the pantothenate kinase (PanK) enzyme present in the cell. PanK catalyzes the first step of CoA biosynthesis, namely the ATP-dependent phosphorylation of pantothenic acid (2) to form 4'-phosphopantothenic acid (P-Pan, 6) (Figure 3A). This reaction is unique because it is catalyzed by three distinct types of PanK, referred to as type I, type II, and type III, respectively. These different PanK types can be distinguished based on their sequence, structure, the extent to which they experience feedback inhibition by CoA, and importantly, their ability to act on pantothenamides as alternative substrates (Brand and Strauss, 2005; Hong et al., 2006; Strauss, 2010; Strauss et al., 2010; Yang et al., 2008). Only type I and II PanKs (PanK_I and PanK_{II})

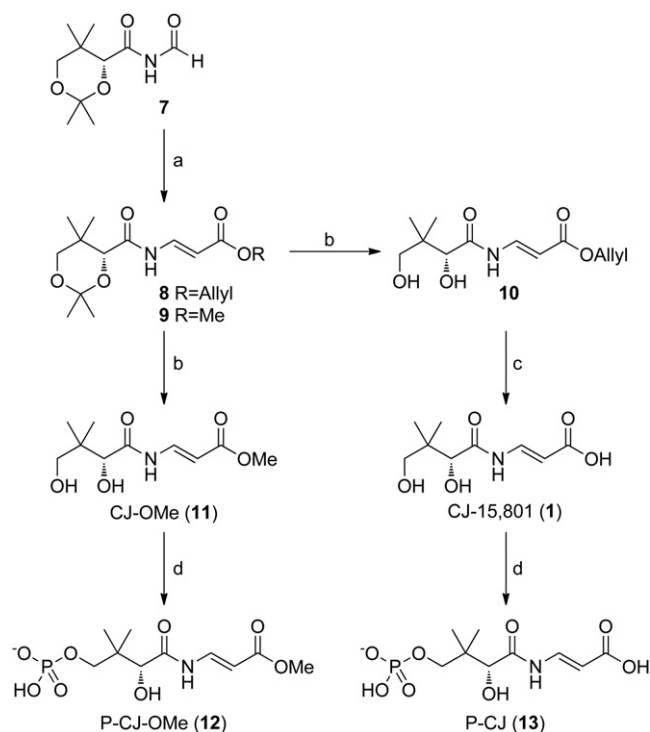


Figure 2. Synthesis of CJ-15,801, Its Methyl Ester and Their Respective Phosphorylated Versions

The respective reaction conditions are as follows: (a) Allyl- or methylacetyltriphenylphosphonium bromide, Et₃N, toluene, 90°C, 75% (Villa et al., 2007); (b) BiCl₃, H₂O, CH₃CN, room temperature, 5 hr, 75%; (c) Pd(PPh₃)₄, pyrrolidine, THF, 81%; (d) SaPanK, ATP, MgCl₂, Tris-HCl (pH 7.5), 98% (for **12**); 79% (for **13**).

See also Figure S3.

phosphorylate pantothenamides, thereby allowing the formation of CoA antimetabolites. Organisms like *Pseudomonas aeruginosa* that have type III PanK (PanK_{III}) enzymes that exclude these compounds from their active sites are therefore refractory to the effects of *N*-pentylpantothenamide and similar analogs (Balibar et al., 2011). This suggests that the basis for CJ-15,801's unique specificity for *S. aureus* and *P. falciparum* may also be based on the type specificity of their PanKs, both of which have been characterized as atypical type II enzymes (Hong et al., 2006; Leonardi et al., 2005; Spry et al., 2010).

In this study, we set out to identify the target of CJ-15,801's antibiotic action in bacteria, to elucidate its mechanism of action, and to establish the basis for its specificity. Our results reveal that CJ-15,801 acts as an antimetabolite by using the first enzyme of the CoA biosynthesis as gateway to the pathway, after which it inhibits the second CoA biosynthetic enzyme, phosphopantothenoylcysteine synthetase (PPCS). This mode of action is reminiscent of the sulfonamide antibiotics, which block folic acid biosynthesis using a similar strategy. However, contrary to expectations, detailed analysis of the inhibition mechanism failed to provide any evidence of irreversible inhibition. Instead, our results show that CJ-15,801 is transformed into a tight-binding mimic of the PPCS enzyme's natural reaction intermediate, a mechanism also utilized by other known natural

product inhibitors of adenylyating enzymes, such as ascamycin and mupirocin (May et al., 2005; Pope et al., 1998). Taken together, these findings not only provide insight into the basis of CJ-15,801's antibiotic action, but also suggest a new and potentially general strategy for the development of synthetase inhibitors with in vivo efficacy.

RESULTS

Synthesis of CJ-15,801 and Its Esters

The synthesis of CJ-15,801 and its related analogs presents several challenges, the first of which relates to the preparation of the *N*-acyl vinylogous carbamic acid moiety. In fact, several groups have used the synthesis of CJ-15,801 to showcase new methodologies developed specifically for the preparation of this functionality (Han et al., 2004; Lee et al., 2006; Nicolaou and Mathison, 2005). However, we found these methods to be unsuitable for this study as they are either optimized for small-scale synthetic preparations, or led to the preferential formation of the unwanted (*Z*)-double bond configuration. We therefore utilized the more recent method of Villa et al., which installs the required *N*-acyl vinylogous carbamic acid moiety mainly with an (*E*)-configuration via Wittig-type chemistry, for preparation of the protected esters **8** and **9** (Figure 2) (Villa et al., 2007). A second challenge derives from the sensitivity of the *N*-vinyl amide moiety to both acid and base, which severely restricts the options for the protection and deprotection of the synthetic intermediates. In this case, established protocols that make use of neutral conditions were used to remove the acetal protecting groups from **8** and **9** to, respectively, obtain CJ-15,801's allyl (**10**) and methyl (**11**) esters, and to remove the allyl ester from **10** to provide CJ-15,801 itself. The (*Z*)-configured analog of CJ-15,801 (**Z-1**) was obtained by similar deprotection of the minor constituent of the Wittig coupling reaction product mixture.

Recently, an updated report of the Wittig-based synthesis of CJ-15,801 appeared in which several other options for deprotection of its carboxyl group are also provided (Sewell et al., 2011).

A Bacterium's Susceptibility to CJ-15,801 Correlates with Its PanK Type

The original Pfizer discovery group found that in standard susceptibility tests conducted using cation adjusted Mueller-Hinton broth as growth medium CJ-15,801 is uniquely and peculiarly selective for *S. aureus*, with none of the other organisms tested showing inhibition at 100 µg/ml (460 µM) (Sugie et al., 2001). These resistant organisms included both Gram-positive (*Staphylococcus*, *Enterococcus*, and *Streptococcus* spp.) and Gram-negative (*H. influenzae*, *Moraxella catarrhalis*, and *E. coli*) bacteria, indicating that cell envelope type alone does not determine selectivity. However, the panel of test organisms also comprised bacteria expressing all three known pantothenate kinase (PanK; Figure 3A) types: the enterococci, streptococci, *H. influenzae*, and *E. coli* are known or predicted to have PanK_I enzymes, while *M. catarrhalis* is predicted to have a PanK_{III} (Yang et al., 2006). Importantly, the staphylococci are the only known bacteria to have an active PanK_{II}, suggesting that the presence of this PanK type is a prerequisite for inhibition by CJ-15,801.

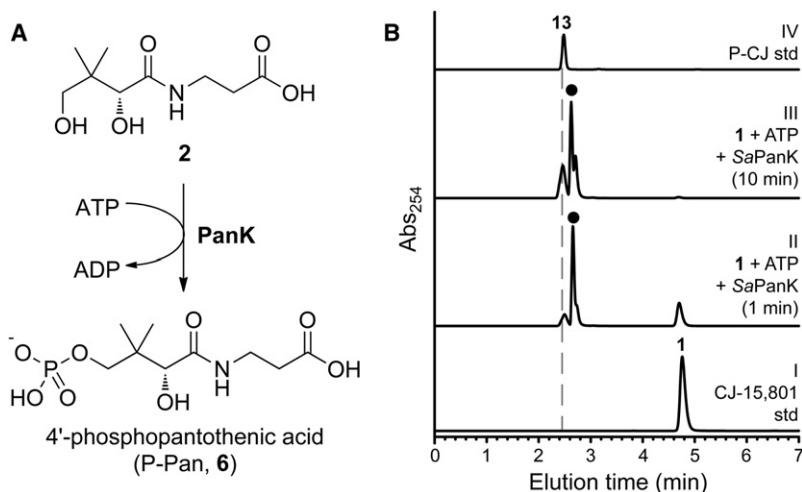


Figure 3. Evaluation of PanK as a Potential Gatekeeper to CJ-15,801's Inhibitory Action

(A) The ATP-dependent phosphorylation of pantothenic acid (**2**) catalyzed by PanK enzymes.

(B) HPLC analysis of the putative ATP-dependent phosphorylation of CJ-15,801 by SaPanK. The traces represent: I, a synthetically prepared standard of CJ-15,801 (**1**); II, a reaction mixture containing CJ-15,801, ATP and SaPanK that had been incubated for 1 min; III, the same after 10 min of incubation; and IV, a synthetic P-CJ (**13**) standard. The peak labeled with (●) represents ATP and ADP.

See also Table S2.

To test this hypothesis, we repeated the CJ-15,801 susceptibility tests against a panel of organisms representing all combinations of cell envelope and PanK type. Since the original tests were conducted in growth medium rich in pantothenic acid, these experiments were conducted in 1% tryptone (that contains essentially no pantothenic acid) instead to exclude any potential antagonistic effects that the presence of the vitamin could have on inhibition. The results show that the PanK_{II}-containing *S. aureus* (MRSA strain TCH1516) was the most sensitive to the inhibitory effects of CJ-15,801, showing an MIC of 15 μ M (Table S1 available online). This value is 2-fold lower than the lowest MIC reported in the previous susceptibility tests, suggesting that pantothenate does affect inhibition similar to what was seen in the experiments with malaria parasites (Saliba and Kirk, 2005). Moreover, under these test conditions some of the other organisms (most notably *P. aeruginosa*) also showed low levels of inhibition (MIC \sim 60 μ M).

To determine which aspects of CJ-15,801's structure are required for inhibition, we evaluated the inhibitory activity of the (Z)-configured analog (**Z-1**) and CJ-15,801's methyl ester (CJ-OMe, **11**) against *S. aureus*. Neither compound showed any inhibition, indicating that the configuration of the double bond and the availability of the free carboxylate of CJ-15,801 are both important determinants for its mechanism of inhibition.

Only PanK_{II} Enzymes Accept CJ-15,801 as Substrate

To confirm that the observed inhibition results can indeed be correlated with PanK type and activity, we performed in vitro activity analyses using purified PanK enzymes. Based on the inhibition results, we first used the most likely candidate, the PanK_{II} enzyme from *S. aureus* (SaPanK_{II}), to determine if it converts CJ-15,801 to phospho-CJ,15,801 (P-CJ, **13**) when incubated with ATP. High-performance liquid chromatography (HPLC) analysis of the reaction mixture confirmed this to be the case, based on the time-dependent formation of P-CJ (Figure 3B). Next, the activity of the PanK_I from *E. coli* (EcPanK_I), SaPanK_{II}, and the PanK_{III} from *P. aeruginosa* (PaPanK_{III}) toward CJ-15,801 were fully characterized kinetically. The resulting data indicate that EcPanK_I and PaPanK_{III} only show activity toward pantothenic acid and not CJ-15,801;

moreover, neither enzyme was inhibited by 100 μ M CJ-15,801 (Table S2). However, SaPanK_{II} shows little distinction between CJ-15,801 and pantothenic acid, exhibiting

specificity constants (k_{cat}/K_m) of $13.8 \pm 4.2 \text{ mM}^{-1} \cdot \text{s}^{-1}$ and $30.2 \pm 8.7 \text{ mM}^{-1} \cdot \text{s}^{-1}$ for the two compounds, respectively, with the difference being mainly due to an elevated K_m value. The enzyme also acts on CJ-OMe, indicating that the lack of inhibition seen for this analog is due to effects downstream of PanK.

Taken together, these results indicate that PanK acts as a gatekeeper to the inhibitory effects of CJ-15,801 in *S. aureus*.

CJ-15,801's Antistaphylococcal Activity Is Affected by Pantothenic Acid and Pantetheine

The observation that *S. aureus*'s susceptibility to inhibition by CJ-15,801 is apparently affected by pantothenic acid (**2**), as well as the finding that SaPanK_{II} accepts both the inhibitor and the vitamin as substrates, led us to perform checkerboard assays to quantify these effects (Figure 4A). The same assay was also conducted with pantetheine (**17**), the precursor to the CoA salvage pathway that bypasses the PPCS and phosphopantothenoylcysteine decarboxylase (PPCDC) enzymes (Strauss, 2010; Strauss et al., 2010) (Figure 4B). The results show that the presence of either compound reduces the potency of CJ-15,801, most likely through competition with SaPanK_{II}. However, their interaction with the natural product is complex, since increasing the concentration of either compound above a certain level (\sim 7.5 μ M for **2**, and \sim 15 μ M for **17**) leads to inhibition being reestablished. While the basis for this observation is currently unknown, the results confirm that the point of CJ-15,801's inhibitory action is a process dependent on pantothenic acid (or pantetheine).

Pantothenamides Increase the Potency of CJ-15,801's Antistaphylococcal Activity

Previous studies have shown that treatment of *S. aureus* with N5-Pan (and its analog, N-heptylpantothenamide, N7-Pan) results in growth inhibition by formation of inactive carrier proteins (Figure 1E) (Leonardi et al., 2005; Zhang et al., 2004). To determine if the points of action of the pantothenamides and CJ-15,801 overlap, a checkerboard assay with N5-Pan (**4**) and CJ-15,801 was performed in 1% tryptone media (Figure 4C). The results show that when combined, CJ-15,801 and N5-Pan exhibited significantly reduced MICs of 3.75 μ M and \sim 1.0 μ M,

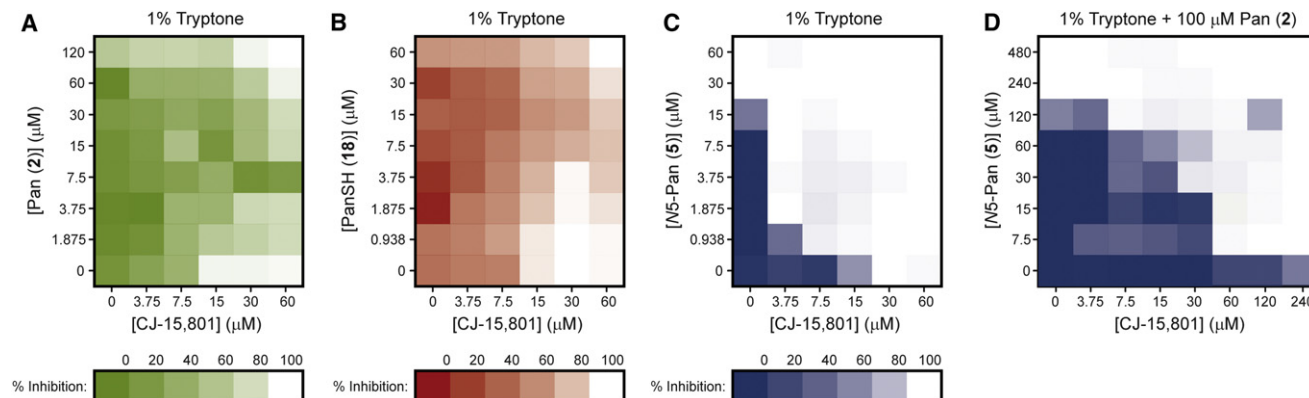


Figure 4. Synergism in the Antibacterial Action of CJ-15,801 and N5-Pan

(A) Checkerboard assay of the growth inhibition of *S. aureus* by CJ-15,801 (**1**) when grown in the presence of pantothenic acid (**2**) in 1% tryptone shows that increasing the amount of vitamin (up to a certain concentration) reverses the inhibition. MIC value for CJ-15,801 is 15 μ M.

(B) As for (A), but with pantetheine (**17**) added instead of pantothenic acid.

(C) Checkerboard assay of the growth inhibition of *S. aureus* grown in 1% tryptone by CJ-15,801 (**1**) and N5-Pan (**4**) demonstrates the synergism between these compounds (FICI < 0.5). MIC value for N5-Pan is 30 μ M.

(D) As for (C), but determined in the presence of 100 μ M pantothenic acid (**2**), demonstrating that the combination of CJ-15,801 and N5-Pan can overcome the antagonism caused by an excess of the natural substrate of the CoA biosynthetic pathway, but at the expense of converting the synergism to an additive effect (0.5 < FICI < 1.0).

See also Tables S1 and S3.

respectively, with a fractional inhibitory concentration index (FICI) of 0.25, indicating synergism (Table S3). Importantly, when the same assay was performed in the presence of 100 μ M pantothenic acid, the inhibition was not as adversely affected as in the case of the individual compounds (Figure 4D). Instead, the MIC values were slightly elevated and the previously observed synergism was converted to an additive inhibitory effect (FICI ~0.5–1.0) (Table S3). This finding suggests that CJ-15,801 and N5-Pan does not have the same mode of action and indicates that in combination these compounds can counter the antagonism caused by pantothenic acid.

Synthesis of the 4'-Phosphates of CJ-15,801 and Its Methyl Ester

The discovery that SaPanK phosphorylates both CJ-15,801 and CJ-OMe (**11**) provided us with a convenient biocatalytic method by which their 4'-phosphorylated versions could be prepared. P-CJ (**13**) and its methyl ester, **12** (P-CJ-OMe), were therefore obtained by milligram-scale biotransformations using recombinant SaPanK and ATP, followed by purification by either preparative HPLC (for P-CJ) or solid-phase extraction (SPE) (for P-CJ-OMe) (Figure 2).

PPCS Accepts P-CJ as Substrate and Is Then Inhibited by It

With the knowledge that CJ-15,801 can be converted to P-CJ within *S. aureus*, we set out to determine if PPCS, the next enzyme in the pathway, is the target for the antibiotic's inhibitory action. PPCS catalyzes the condensation of P-Pan (**6**) with L-cysteine to form 4'-phosphopantothencysteine (PPC, **15**) using a two-step acyl transfer mechanism common to most synthetase (C-N ligase) enzymes, including all the amino acid tRNA synthetases and the adenylation domains of the modular nonribosomal peptide synthetases (NRPSs) (Figure 5A)

(Schimmel et al., 1998; Sieber and Marahiel, 2005). While all known PPCSs follow this general scheme, bacterial enzymes are unique in that they use CTP instead of ATP as nucleotide source for the activation reaction, and therefore form 4'-phosphopantothencyl-CMP (P-Pan-CMP, **14**) as intermediate (Kupke, 2002, 2004; Manoj et al., 2003; Stanitzek et al., 2004; Strauss, 2010; Strauss et al., 2001).

In most bacteria PPCS activity is located on one domain of the bifunctional CoaBC protein (which also carries PPCDC activity), although monofunctional PPCS enzymes do occur in certain enterococci (such as *Enterococcus faecalis* [Yao et al., 2009]) and streptococci. Among all bacterial PPCS enzymes the PPCS activity of *E. coli*'s bifunctional CoaBC protein is by far the best studied: its mechanism has been established through trapping and isolation of P-Pan-CMP (**14**), and the structure of the N210D mutant with the trapped intermediate **14** bound in the active site has been determined (Kupke, 2002, 2004; Stanitzek et al., 2004). Moreover, many of these studies were performed using the separate PPCS domain (*EcPPCS*) expressed and purified on its own, showing that the two activities of the bifunctional CoaBC protein are independent. This conclusion is also supported by kinetic isotope studies of the PPCDC activity of *E. coli*'s CoaBC (Strauss and Begley, 2001). We therefore decided to use the *EcPPCS* domain to perform the initial tests on the interaction of PPCS and P-CJ.

To determine if P-CJ is accepted as an alternate substrate by PPCS and forms the corresponding P-CJ-CMP intermediate **16** (Figure 5B), mixtures of P-CJ and CTP were incubated with increasing concentrations of *EcPPCS*. A clear correlation between the rate of pyrophosphate release and enzyme concentration was evident in such reactions (Figure 5C). Moreover, HPLC analysis of the reaction mixture containing the highest *EcPPCS* concentration (24 μ M) showed the formation of a peak absent in native reaction mixtures, or in mixtures

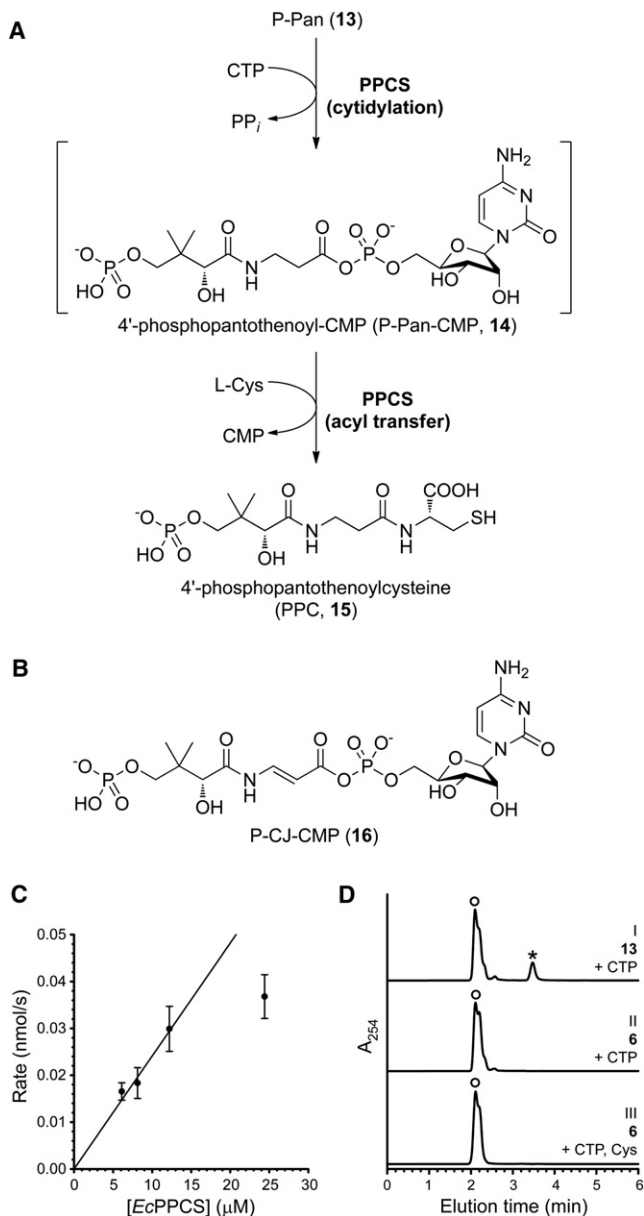


Figure 5. Evaluation of PPCS Activity with P-CJ (13) as Substrate

(A) The reaction catalyzed by PPCS, showing the two steps of its mechanism and the P-Pan-CMP (14) reaction intermediate.

(B) The structure of P-CJ-CMP (16) resulting from the putative cytidylation of P-CJ (13) by PPCS.

(C) The rate of pyrophosphate release from a reaction mixture containing P-CJ (13), CTP, and EcPPCS correlates with enzyme concentration. Experiments were run in duplicate; the shown data points are the average of duplicate assays (error bars indicate the SD).

(D) HPLC analysis of a reaction mixture containing P-CJ (13), CTP, and EcPPCS (24 μM) (trace I) show the formation of a new peak (indicated with an asterisk) that represents P-CJ-CMP (16) based on LC-MS analysis. This peak is not present when P-CJ is replaced with P-Pan (6) (trace II) or in native reaction mixtures containing P-Pan, CTP and L-cysteine. Note that the retention time of pure P-CJ is ~2.4 min (see Figure 2B). The broad peak labeled with (O) represents CTP and CMP.

See also Figure S1.

containing P-Pan (6) instead of P-CJ, suggesting the formation of P-CJ-CMP (Figure 5D). Note that P-Pan-CMP is usually not observed under these conditions, as was previously reported (Kupke, 2002, 2004). Liquid chromatography-tandem mass spectrometry (LC-MS) analysis was subsequently conducted on the same mixture. While the P-CJ-CMP-derived molecular ion was not observed, the corresponding mass spectrum did show mass peaks that are in agreement with the fragmentation of P-CJ-CMP (Figure S1). The same experiment was subsequently repeated with the bifunctional CoaBC protein from *S. aureus* (SaCoaBC). A similar result was obtained, although the apparent rate of conversion of P-CJ into P-CJ-CMP was significantly slower than for EcPPCS (Figure S1).

In combination, these results indicate that P-CJ is accepted as an alternate substrate by PPCS, which cytidylates its carboxylate to form P-CJ-CMP.

PPCS Transform P-CJ into P-CJ-CMP, which Inhibits Its Activity

Subsequent activity analysis of PPCS in the presence of P-CJ, CTP, and L-cysteine failed to show catalytic turnover. Moreover, when P-CJ was added to PPCS reaction mixtures containing the enzyme's native P-Pan substrate, the rate of the reaction was reduced compared to mixtures without it, suggesting inhibition by P-CJ. To confirm that such inhibition is dependent on the reaction catalyzed by PPCS, an inhibition screen was performed in which CJ-15,801, CJ-OMe, P-CJ, or P-CJ-OMe was added to native PPCS reaction mixtures at a concentration of 100 μM. The results showed that among these compounds, only P-CJ inhibited EcPPCS (data not shown). The lack of inhibition by P-CJ-OMe indicated that the free carboxylate group is required for inhibition, while the inability of CJ-15,801 to affect enzyme activity highlights the necessity of the phosphate group for binding. Taken together with the results described above, these findings reveal PPCS as CJ-15,801's target of inhibitory action, which is achieved through formation of P-CJ-CMP 16 as an apparent dead-end inhibitor.

Kinetic Characterization Reveals P-CJ-CMP as a Tight-Binding Inhibitor of PPCS

Inhibition by P-CJ-CMP could potentially occur by either of the proposed irreversible inhibition mechanisms (Figures 1C and 1D), or by a completely unrelated mechanism. To elucidate the actual mechanism of inhibition, detailed kinetic analyses were performed. First, dose-response curves were used to evaluate the inhibition of the cytidyl-transfer reaction catalyzed by EcPPCS. The resulting IC_{50} value of 2.66 ± 0.16 μM, determined using saturating concentrations of CTP and 100 μM P-Pan (note that EcPPCS experiences substrate inhibition, see Figure S2), was less than 10-fold the concentration of enzyme used in these assays (240 nM). This indicated that P-CJ-CMP acts as either a tight-binding or irreversible inhibitor of EcPPCS (Copeland, 2000). The inhibition of EcPPCS was next studied by the progress curve method. The resulting curves increased in a linear fashion, showing a decreased rate at increased concentrations of P-CJ (Figure 6A). Surprisingly, this indicated that the inhibition was tight binding and not irreversible (which would have led to the steady-state rates approaching zero) as predicted (Copeland, 2005). This finding was confirmed by showing that

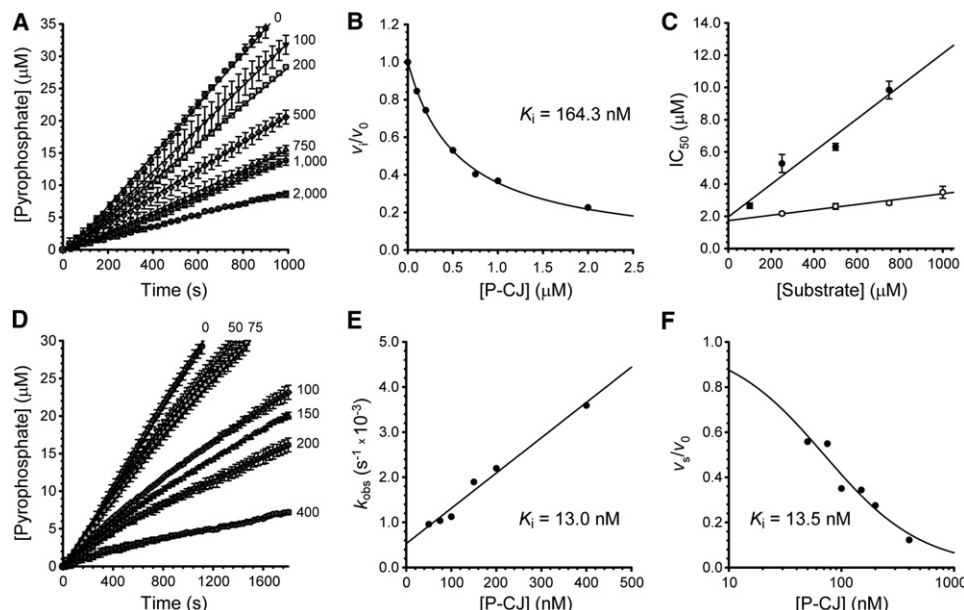


Figure 6. Kinetic Characterization of the CJ-15,801-Based Inhibition of PPCS

(A) Progress curves analysis for the inhibition of EcPPCS in the presence of increasing concentrations of P-CJ (**13**), indicated in nM next to each curve.

(B) Plot of the fractional activity (initial velocity v_i relative to the inhibited velocity v_0), as determined from the progress curves in (A), against inhibitor concentration. The indicated K_i value is determined by fitting the data to the Morrison and Cheng-Prusoff equation.

(C) Determination of the inhibition modality of EcPPCS by P-CJ (**13**) by calculation of the IC_{50} values in the presence of increasing concentrations of P-Pan (**6**) (●), and CTP (○).

(D) Progress curves analysis for the inhibition of SaCoaBC in the presence of increasing concentrations of P-CJ (**13**), indicated in nM next to each curve.

(E) Plot of the first order rate of inactivation constants (k_{obs}), as determined from the data presented in (D), against inhibitor concentration. The indicated K_i value is determined by fitting the data to the equation for a straight line.

(F) Plot of the fractional activity (steady-state velocity v_s relative to the inhibited velocity v_0), as determined from the progress curves in (D), against inhibitor concentration. The indicated K_i value is determined by fitting the data to a Langmuir isotherm.

All progress curve analyses were performed in triplicate (error bars represent the SD).

See [Supplemental Experimental Procedures](#) for details on calculations, as well as [Figure S2](#) for the determination of EcPPCS and SaCoaBC kinetic parameters.

removal of the inhibitor by gel filtration was sufficient to restore the activity of a sample of EcPPCS that had been pretreated with P-CJ and CTP.

The K_i^{app} (apparent inhibition constant) was subsequently calculated by plotting the fractional activity versus inhibitor concentration, plotting the data to the Morrison equation ([Figure 6B](#)), and converting the obtained value to the true K_i by applying the appropriate Cheng-Prusoff equation ([Copeland, 2000, 2005](#)). The mode of inhibition was established using a method specifically developed for tight-binding inhibitors in which IC_{50} values are determined at a fixed enzyme concentration, but in the presence of increasing concentrations of either P-Pan (**6**) or CTP ([Figure 6C](#)). A linear increase in IC_{50} values with increasing concentration of P-Pan but not CTP indicates that inhibition is competitive toward P-Pan but noncompetitive toward CTP ([Copeland, 2000, 2005](#)). This observation agrees with previous studies of the *E. faecalis* and human PPCS enzymes that determined an ordered Bi Uni Bi Ping-Pong kinetic mechanism with CTP binding first, followed by P-Pan (**6**) ([Yao and Dotson, 2009; Yao et al., 2009](#)). In this manner, a K_i of 164.3 nM was determined for P-CJ's inhibition of EcPPCS.

While EcPPCS is a convenient and well-studied model to use for characterization of CJ-based inhibition, *E. coli* is not affected

by CJ-15,801 due to the gatekeeping activity of its PanK ([Tables S1 and S2](#)). We therefore performed the same kinetic analysis on SaCoaBC, which is expected to be the natural target for CJ-15,801's observed antistaphylococcal action. A progress curve analysis similar to that conducted on EcPPCS showed that SaCoaBC experiences time-dependent inhibition, since the curves showed a fast initial velocity (v_i) phase and a slower steady-state velocity (v_s) phase ([Figure 6D](#)). The first order rate of inactivation constants (k_{obs}) were subsequently determined and plotted against the inhibitor concentration. The resulting plot ([Figure 6E](#)) showed a linear relationship between k_{obs} and $[I]$, which points to a one-step inhibition mechanism ([Copeland, 2005](#)). However, it is more likely that the true mechanism consists of two steps, with P-CJ **13** binding first in a reversible manner, followed by the slow formation of P-CJ-CMP. Such a mechanism would be kinetically indistinguishable from a one-step mechanism.

The K_i value for the inhibition of SaCoaBC by P-CJ-CMP can be determined from the slope and y-intercept of the linear plot shown in [Figure 6E](#). The K_i value can also be calculated by using the progress curves to determine the steady-state velocity (v_s) at each inhibitor concentration; a plot of the fractional activity against inhibitor concentration yields an isotherm curve with the K_i at its midpoint ([Figure 6F](#)) ([Copeland, 2005](#)). In this manner,

K_i values of 13.0 and 13.5 nM were determined, respectively. These values are nearly an order of magnitude lower than that determined for EcPPCS, clearly showing that the nature of the actual target protein also plays an important role in the extent of inhibition. Taken together, these data show that P-CJ-CMP acts as a tight-binding inhibitor of PPCS enzymes.

Analysis of the Mechanistic Basis for the Tight-Binding Inhibition of P-CJ-CMP

The close structural homology between P-Pan-CMP (**14**) and P-CJ-CMP (**16**), and the fact that both compounds contain reactive acyl phosphate moieties, raises a question regarding the mechanistic basis for the inhibition by P-CJ-CMP. We considered three possible explanations: first, inhibition is based on differences in the electrophilicity of the carbonyl carbon of the acyl phosphate moieties of P-Pan-CMP and P-CJ-CMP, respectively; second, inhibition is caused by the two compounds having different binding modes in the active site, due to the structural nature of the planar *N*-acyl vinylogous carbamate functionality of P-CJ-CMP; and third, inhibition is caused by P-Pan-CMP and P-CJ-CMP having different effects on any conformational changes that occur during catalysis through stabilization of the protein's quaternary structure. While the significant synthetic effort that is required to prepare P-Pan-CMP and P-CJ-CMP precluded a direct experimental comparison of their respective reactivities, we were able to perform tests to assess whether the latter two proposed mechanisms contribute to inhibition.

To establish if P-Pan-CMP (**14**) and P-CJ-CMP (**16**) have different binding modes, we used the only available structure of a PPCS enzyme with its intermediate bound, that of the EcPPCS Asn210Asp mutant with P-Pan-CMP bound in the active site (PDB ID: 1U7Z). This mutant, which accumulates sufficient amounts of the intermediate to have allowed direct confirmation of its identity and structure (Kupke, 2004; Stanitzek et al., 2004), is apparently unable to catalyze the second step of the PPCS reaction. However, the molecular basis for this catalytic disability remains speculative since no PPCS structure with cysteine bound has been determined thus far. Nonetheless, the mutation clearly results in tightly bound P-Pan-CMP in the enzyme's active site.

We constructed a model of the native enzyme by reversing the Asn210Asp mutation in the crystal structure and used it to dock P-CJ-CMP (**16**) in the active site using 150 starting conformations to ensure sufficient conformational space was sampled considering the complexity of the molecule. The highest scoring docked pose of P-CJ-CMP very closely mimics the pose of the cocrystallized P-Pan-CMP in the crystal structure (Figure 7A), and facilitates all the same hydrogen bonding interactions while maintaining a near planar geometry across the *N*-acyl vinylogous carbamate moiety (Figure 7B). This suggests that the basis for inhibition by P-CJ-CMP is not due to it having a different binding mode, or taking on a potentially unreactive conformation.

Members of the ANL superfamily of adenylating enzymes, such as the adenylation domains of the NRPSs, use a large domain rotation event to facilitate the catalysis of their two-step reactions (Gulick, 2009). While it is currently unknown whether PPCS enzymes, which belong to the ribokinase family, undergo similar large conformational changes during catalysis, the determined crystal structures of the *E. coli* and human

proteins show that they occur as dimers, with the dimer interface partially occluding the active site (Manoj et al., 2003; Stanitzek et al., 2004). To evaluate the effect of different ligands on the enzyme's overall stability, the melting temperatures (T_m) of the EcPPCS protein in the presence of its native substrates or the inhibitor were determined by following the heat-induced denaturation of these mixtures by circular dichroism (CD). The results show that the T_m increases from 47.7°C (for the free enzyme) to 49.7°C (for the enzyme bound to CTP) to 54.3°C (for the enzyme bound to P-Pan-CMP, formed in situ from P-Pan and CTP), highlighting the many stabilizing interactions the protein has with its native ligands (Figure 7C). Importantly, the T_m of EcPPCS bound to P-CJ-CMP (formed in situ from P-CJ and CTP) shows an even larger increase to 57.3°C. When the same experiment was conducted with the bifunctional SaCoaBC, the protein showed increased stability compared to EcPPCS (CoaBC proteins exist as higher order oligomers, usually dodecamers [Manoj et al., 2003]), but only small differences in the T_m values for the protein in the absence and presence of its native ligands. However, the T_m showed an impressive improvement from ~65°C to 85°C for the proteins bound to P-Pan-CMP and P-CJ-CMP, respectively (Figure 7D). Taken together, these findings indicate that the binding of the conformationally more rigid ligand **16** results in an increased stabilization of the PPCS oligomers and the trapping of the ligand in the active site. This stabilization, which may be due to interactions between the ligand and residues of the adjacent monomer (such as Lys289, see Figure 7B) contained in a disordered loop that partially covers the entrance to the active site (Figure 7E), is therefore most likely an important contributor to the mechanism of inhibition by P-CJ-CMP.

DISCUSSION

One of the biggest obstacles to elucidation of the CJ-15,801 mode of action is scarcity of the natural product. The original discoverers shared the bulk of the isolated material with the authors of a malaria parasite inhibition study (Spry et al., 2008), but new stocks are unlikely to be obtained in this manner since the CJ-producing *Seimatosporium* strain can currently not be traced due to closure of the laboratory in which it was characterized (Y. Sugie, personal communication). New developments in the synthesis of CJ-15,801 have certainly improved the situation, but the unique sensitivity of the *N*-acyl vinylogous carbamic acid functionality still presents a significant challenge to the synthesis of this antibiotic.

The original finding that CJ-15,801 is highly selective in its antibiotic action, affecting only *S. aureus* strains among a range of other Gram-positive bacteria including *Streptococcus* and *Enterococcus* spp. (Sugie et al., 2001), provoked curiosity in regards to its mechanism of action. Here, we show that the primary reason for this selectivity is the substrate specificity of the host organism's PanK enzyme. Only the PanK_{II} of *S. aureus* accepts CJ-15,801 and phosphorylates it, thereby allowing it to enter the CoA biosynthetic pathway. Interestingly, SaPanK_{II} is the only known active bacterial representative of a type II PanK; all other examples occur in eukaryotes. However, an earlier study showed that CJ-15,801 does not inhibit rat hepatoma cells, suggesting that typical eukaryotic PanKs do not act as

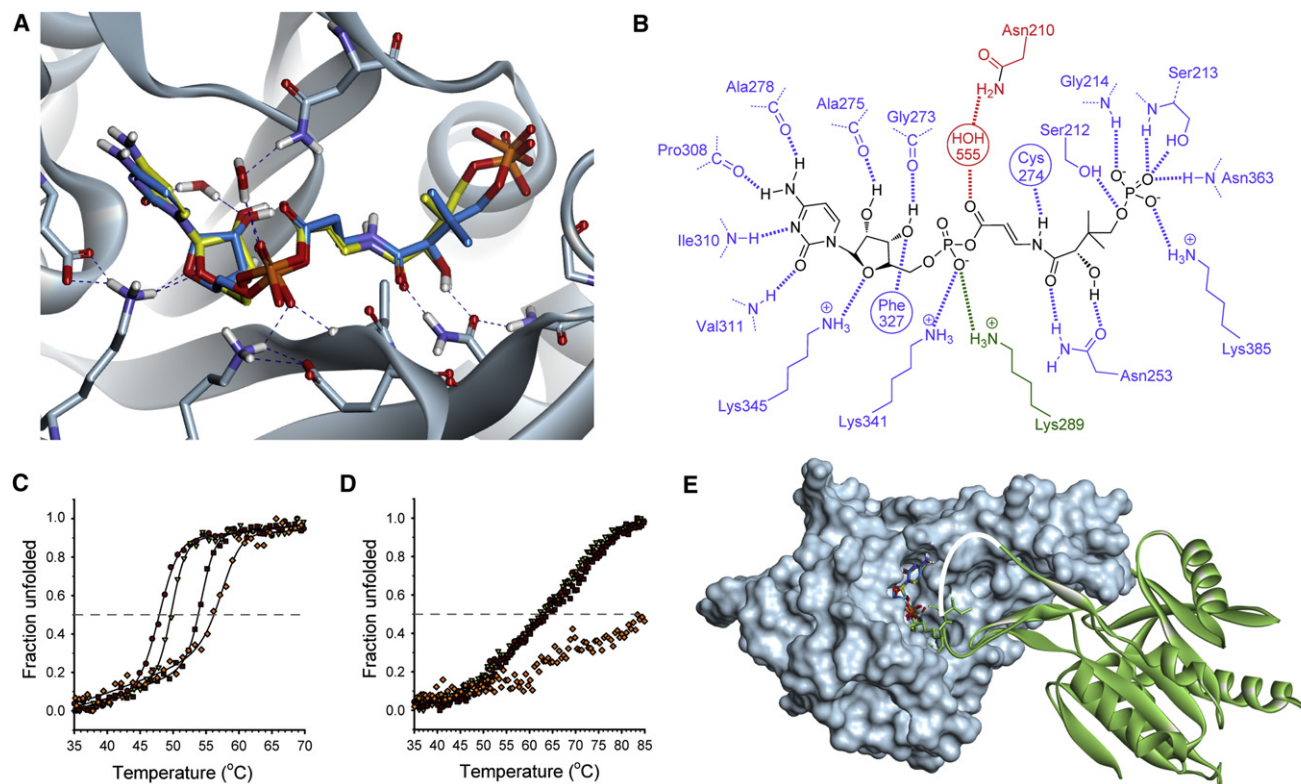


Figure 7. Structural Basis for the Tight-Binding Inhibition of the CJ-15,801-Derived Inhibitor

(A) Structure of the P-CJ-CMP inhibitor **16** (stick structure with carbon atoms in yellow) modeled and overlaid on that of the P-Pan-CMP intermediate **14** (stick structure with carbon atoms in blue) bound in the active site of native EcPPCS. The model was created from the crystal structure of EcPPCS Asn210Asp with cocrystallized P-Pan-CMP **14** bound (PDB: 1U7Z) by reversing the mutation, and docking P-CJ-PMP. The highest scoring pose of P-CJ-CMP closely resembles that of P-Pan-CMP and similarly facilitates all hydrogen bonding interactions observed for P-Pan-CMP. Only selected residues are shown for clarity.

(B) Schematic view of polar interactions between P-CJ-CMP and EcPPCS. Residues from monomer A are in blue and those from monomer B in green. The key interaction between Asn210 and the acyl phosphate carbonyl, mediated via a bridging water molecule, is shown in red.

(C) Heat-induced protein melting curves for EcPPCS. The four curves represent from left to right: the free protein (●); protein with MgCTP (▼); protein with MgCTP and P-Pan (**2**) (■); and protein with MgCTP and P-CJ (**13**) (■ ■ ■). The curves were determined by following changes in the protein's secondary structure by circular dichroism.

(D) Heat-induced protein melting curves for SaCoaBC determined as for EcPPCS in (B).

(E) Structure of the EcPPCS dimer (PDB: 1U7Z) with one monomer shown as a solvent-accessible surface (in cyan) and the other as ribbon structure (in green). The overlaid P-Pan-CMP and P-CJ-CMP stick structures are shown docked in the active site. Note that residues 291–298, which form part of a loop (shown in white) that cover the active site, is normally disordered and is absent in all crystal structures of PPCS enzymes (Manoj et al., 2003; Stanitzek et al., 2004).

See also Figure S4.

gateways to its antibiotic action (Saliba and Kirk, 2005). Such a conclusion is supported by the results of a structure-activity relationship study of the inhibition of EcPanK_I and the PanK_{II}s from *Aspergillus nidulans*, *Mus musculus* (mouse), and *S. aureus* by the pantothenamides, which showed a clear differentiation between eukaryotic PanK_{II}s and SaPanK_{II}, and even between the eukaryotic PanK_{II}s themselves (Virga et al., 2006). The varied selectivity of PanK_{II}s have clearly not been fully explored, since *P. falciparum* (which is also sensitive to inhibition by CJ-15,801) is also predicted to have a PanK_{II} (Spry et al., 2010).

The evolution of CJ-15,801 as a natural product that specifically targets the *S. aureus* CoA biosynthetic pathway may reflect this organism's unique redox physiology. Like some other Gram-positive bacteria, including *Bacillus anthracis* (Nicely et al., 2007), *S. aureus* does not contain glutathione but instead relies on the sacrificial oxidation of CoA and a specific NADPH- and flavin-

dependent CoA disulfide reductase (CoADR) enzyme to maintain its intracellular redox balance (delCardayre and Davies, 1998; Mallett et al., 2006). This causes *S. aureus* to maintain high intracellular levels of reduced CoA (Newton et al., 1996), which imparts an additional unique characteristic to SaPanK_{II}: unlike other eukaryotic PanK_{II}s, it is refractory to feedback inhibition by CoA and its thioesters (Choudhry et al., 2003; Hong et al., 2006; Leonardi et al., 2005). The combination of *S. aureus*'s distinctive reliance on CoA biosynthesis and the unique characteristics of its SaPanK_{II} enzyme have seemingly created an ideal target for antibacterial action that was eventually exploited through the production of CJ-15,801.

The interaction between CJ-15,801 and pantothenic acid and its analogs is complex, and warrants further study (Figures 4A and 4B). The observation that inhibition by CJ-15,801 is alleviated in the presence of either pantothenic acid or pantetheine

is expected in light of its determined mode of action; however, it is unclear why the inhibition returns when the concentrations of the vitamin is increased beyond a certain level. It is possible that the susceptibility to CJ-15,801 under these circumstances is due to the high concentrations of pantothenic acid stimulating CoA biosynthesis, as this would result in increased amounts of P-CJ-CMP being formed. The low levels of inhibition seen in the absence of pantothenic acid in organisms such as *P. aeruginosa* that cannot form P-CJ (and which therefore should not experience any inhibition by the mechanism proposed here) is probably due to similar effects on the regulation of pantothenic acid biosynthesis and/or utilization. However, such effects are clearly weak, as they are completely abolished in the presence of increased concentrations of the vitamin.

The finding that CJ-15,801 and members of the pantothenamide class of antibiotics work in a synergistic fashion supports most studies that have indicated that the pantothenamides have a target downstream of CoA biosynthesis (Figure 4C) (Leonardi et al., 2005; Mercer et al., 2009; Thomas and Cronan, 2010; Zhang et al., 2004). Moreover, such a combination can apparently maintain its inhibitory effects even in the presence of pantothenic acid (Figure 4D). This indicates that it is possible to increase the modest antistaphylococcal activity of CJ-15,801 and even counteract the antagonism caused by pantothenic acid by combining it with other appropriate inhibitors, especially those that also affect CoA-based metabolism.

The finding that P-CJ-CMP acts as a tight-binding inhibitor of the PPCS enzyme can be rationalized in light of the findings of previous studies that have shown that nonhydrolyzable mimics of acyl nucleotidylate intermediates are often potent (tight-binding) inhibitors of enzyme activity (Cisar and Tan, 2008; Kim et al., 2003; Schimmel et al., 1998). In fact, this strategy was also successfully applied to PPCS in a study in which the phosphodiester analog of P-Pan-CMP was shown to be a potent inhibitor of the PPCS of *E. faecalis* (Patrone et al., 2009). However, the finding that P-CJ-CMP does not undergo attack by cysteine in spite of having an activated acyl phosphate moiety remains surprising. Of the three possible mechanisms that were considered for the inhibition by P-CJ-CMP, the most likely is that the introduction of the conjugated system in the β -alanine moiety reduces the reactivity of the acyl phosphate carbonyl toward nucleophilic attack. Such a reduced activity could be based on electronic effects, or be due to the potential tautomerization of the carbonyl enamine function of the inhibitor to an enol imine. Such a modification in reactivity has been noted in similar systems, as in the case of the vinylogous carbamate ester that forms as a result of the mechanism of action of the β -lactamase inhibitor clavulanate (and penam sulfones), and which has been reported to be stable toward hydrolysis (Imtiaz et al., 1993). However, structural studies have indicated that this stability is partly due to interactions with active site residues, and that it can be enhanced by manipulation of these interactions (Padayatti et al., 2005, 2006). Our model of P-CJ-CMP docked in the active site of EcPPCS does not show the formation of any new active site-ligand interactions that are not present with P-Pan-CMP, suggesting that such factors are not at play in the inhibition of PPCS by P-CJ-CMP.

Our experiences with the synthetic preparation of CJ-15,801 (Figure 2) indicated that the conjugation provided by the unsatu-

rated β -alanine moiety does deactivate this center. Specifically, all chemical attempts to hydrolyze the methyl esters **9** and **11** en route to **1** proved difficult and inefficient, which necessitated the use of an allyl ester protection strategy that deprotects via nonhydrolytic mechanisms. However, direct evidence for the difference in reactivities between P-CJ-CMP and P-Pan-CMP will have to be obtained through experimentation with model systems; these studies are currently under way.

Nonetheless, the results of the temperature melting curve analyses clearly show that P-CJ-CMP also significantly improves the overall stabilization of PPCS oligomers compared to the natural intermediate P-Pan-CMP, indicating that the stabilization of certain conformations of the enzyme could also be an important factor causing inhibition. The finding that the extent of apparent stabilization is much larger for SaCoaBC than EcPPCS (which is in agreement with the significantly lower K_i observed in the case of the former protein) could be due to the increase in stability being compounded in the bifunctional CoaBC proteins that usually form dodecamers instead of the dimers formed by most PPCS enzymes. We conclude that this stabilization prevents further reaction by cysteine by protecting the potentially reactive P-CJ-CMP intermediate, resulting in its trapping in the active site and the observed inhibition. This analysis is supported by the available EcPPCS structures, which show significant differences in the active site architectures of the CTP (PDB: 1U7W), P-Pan-CMP (PDB: 1U7Z), and CMP-bound (PDB: 1U7O) forms of the enzyme, indicating that the enzyme undergoes significant movement during catalysis.

In conclusion, we have demonstrated that the natural product CJ-15,801 hijacks the CoA biosynthetic pathway, and inhibits its second enzyme by forming a tight-binding inhibitor in situ within the active site. This mechanism is highly reminiscent of that of the sulfonamide antibiotics, which inhibit the biosynthesis of another vitamin—folic acid—in a similar manner. The mechanism is also complementary to that employed by an adenosine sulfamate inhibitor of ubiquitin-like protein conjugation pathways, which also forms a nonhydrolyzable mimic of its target's reaction intermediate in situ (Brownell et al., 2010; Chen et al., 2011). Taken together, these findings provide important new insights into inhibitors that target CoA biosynthesis and CoA-utilizing enzymes. They also highlight an alternative strategy for inhibitor development—one based on the stabilization of certain protein conformations—that may also hold significant potential for drug design efforts targeting other medicinally relevant synthetase enzymes.

SIGNIFICANCE

The antibiotic CJ-15,801 was found to be a selective inhibitor of CoA biosynthesis in *S. aureus* due to the unique selectivity of SaPanK, the first enzyme of the CoA pathway, which currently is the only known example of an active bacterial PanKil enzyme. This demonstrates that the diversity of PanK enzymes can be exploited for selective inhibition or, as in this case, specific gatekeeping functions. The phospho-CJ-15,801 product that forms as a result of the phosphorylation by PanK subsequently acts as a substrate for PPCS, which transfers a cytidyl group to its carboxylate to form P-CJ-CMP. Surprisingly, this reaction does not result

in the formation of an electrophilically reactive intermediate; instead P-CJ-CMP acts as a potent tight-binding inhibitor of the enzyme. The results of temperature-dependent stability studies indicate that this inhibition is at least partly due to stabilization of the interactions between the adjacent monomers in the PPCS dimer, which seemingly prevents the reaction of cysteine—the second substrate in the PPCS reaction—with the activated acyl group of P-CJ-CMP. These findings indicate that the inhibition of synthetase enzymes by nonreactive analogs of their intermediates may have an alternative mechanistic basis in some cases, which is the stabilization of certain structural conformations, and that this should be considered as a potential new strategy for the inhibition of these enzymes. The findings also reveal CJ-15,801 as an antimetabolite of a vitamin biosynthetic pathway, similar to the sulfonamide antibiotics. Finally, we show that the potency of CJ-15,801 is significantly improved in combination with a pantothenamide, a known CoA antimetabolite precursor, confirming that these antimicrobials have different points of action and establishing the potential of drug development strategies that are focused on enzymes involved in CoA biosynthesis and utilization.

EXPERIMENTAL PROCEDURES

See Supplemental Experimental Procedures for full details of all synthetic procedures (including characterization data for all compounds), antibacterial activity assays, procedures for the preparation of proteins, enzyme assays and accompanying data analyses, and protein melting temperature determinations and analysis.

Synthesis of CJ-15,801 and Its Analogs

The inhibitor and its analogs were prepared by modification of published procedures (Figure S3) (Nicolaou and Mathison, 2005; Sewell et al., 2011; Villa et al., 2007).

Inhibition Assays and Analysis

The activity of CJ-15,801 against test strains of *S. aureus*, *Streptococcus agalactiae*, *E. coli*, *P. aeruginosa*, and *Bacillus subtilis* was assessed by MIC assays performed by microbroth dilution in 96-well microtiter plates and turbidometric analysis at OD₆₀₀. The effect of pantothenate and its analogs on the antibiotic activity of CJ-15,801 against *S. aureus* was assessed in a checkerboard assay to calculate FICI indicative of synergy, additivity, indifference, or antagonism (Orhan et al., 2005).

PanK Assay and Data Analysis

Pantothenate kinase activity was determined using a continuous spectrophotometric assay that coupled the production of ADP to the consumption of NADH as described previously (Brand and Strauss, 2005; Strauss and Begley, 2002). All enzyme assays were based on decrease of NADH concentration, as monitored by change in absorbance at 340 nm. An extinction coefficient of 6,220 M⁻¹·cm⁻¹ was used for NADH. Assays were performed in 96-well UV transparent plates (Greiner Bio) and monitored for between 10 min and 1 hr at 25°C using a Perkin-Elmer HTS 7000 Bio-Assay Reader or a Thermo Scientific Varioskan Multimode Reader. For EcPanK_I and SaPanK_{II}, each 320 μ l reaction contained ATP (1.5 mM), MgCl₂ (10 mM), KCl (20 mM), NADH (0.3 mM), phosphoenolpyruvate (0.5 mM), pyruvate kinase (5 units), and lactate dehydrogenase (5 units) in 50 mM HEPES buffer (pH 7.5). For PaPanK_{III}, each 300 μ l contained ATP (5.0 mM), MgCl₂ (1 mM), NH₄Cl (60 mM), NADH (0.5 mM), phosphoenolpyruvate (2.0 mM), pyruvate kinase (2 units), and lactate dehydrogenase (2.75 units) in 100 mM HEPES buffer (pH 7.5). The concentration of pantothenate, CJ-15,801, and other substrate analogs was varied between 6.25 and 200 μ M. Reactions were initiated by addition of SaPanK_{II} (3 μ g), EcPanK_I (3.5 μ g), or PaPanK_{III} (5 μ g). Initial

velocities were calculated for each substrate concentration and fitted to the Michaelis-Menten equation using Prism software (Graphpad) or SigmaPlot 11.0 (Systat software). All measurements were obtained in triplicate.

PPCS Assay and Data Analysis

PPCS assays were performed according to the published procedure (Patrone et al., 2009; Yao et al., 2009). The PPCS reaction was observed in the forward reaction via an enzyme-linked assay in which the pyrophosphate that is released during transfer of CMP from CTP to the substrate is continuously detected; this is achieved using the commercially available pyrophosphate reagent from Sigma-Aldrich (Cat. # P7275). Each vial of the pyrophosphate reagent was resuspended in 4.5 ml of dH₂O. The assays were performed on a Biotek PowerWave microplate spectrophotometer at 37°C. All curve-fitting analyses were performed using SigmaPlot 11.0 (Systat software).

Molecular Modeling

Modeling studies were performed using Accelrys Discovery Studio 3.1 (DS 3.1). The coordinates for EcPPCS Asn210Asp containing P-Pan-CMP as a cocrystallized ligand were obtained from the Protein Data Bank (PDB code: 1U7Z). The structure was optimized prior to any receptor-ligand calculations (full details of the receptor preparation are given in the Supplemental Experimental Procedures). Docking of P-CJ-CMP was accomplished using CDOCKER (Wu et al., 2003), launched from within DS 3.1. Deviations from the default settings included generating 150 starting conformations of the ligands to adequately sample conformational space and 50 poses were selected for simulated annealing. The top scoring pose (CDOCKER_Energy) was visually inspected and found to mimic the binding of the co-crystallized P-Pan-CMP. To ensure that the optimized water bridging the connection between the Asn210 amide side chain and the phosphate of P-Pan-CMP was not biasing the pose found in the docking, the exercise was repeated without this water molecule, which resulted in a nearly identical pose being found. Similarly, docking of P-CJ-CMP in the original structure of the EcPPCS Asn210Asp mutant (1U7Z) again showed that P-CJ-CMP very closely mimics the binding pose of the P-Pan-CMP molecule cocrystallized in the active site (Figure S4).

Protein Melting Temperature Determinations and Analysis

Protein melting curves were determined by measuring the heat-induced unfolding of the PPCS proteins by circular dichroism (CD) at 220 nm in a 0.5 mm cuvette using an Applied Photophysics Chirascan-Plus CD spectrometer. Samples contained the PPCS protein (10 μ M) and MgCl₂ (1 mM) in 50 mM Tris-HCl buffer (pH 7.6) and CTP (150 μ M), CTP and P-Pan (150 μ M each), or CTP and P-CJ (150 μ M each).

SUPPLEMENTAL INFORMATION

Supplemental Information includes four figures, three tables, and Supplemental Experimental Procedures and can be found with this article online at doi:10.1016/j.chembiol.2012.03.013.

ACKNOWLEDGMENTS

We thank the following persons for assistance with various experiments: Leisl Brand for the preparation of the SaCocBC-expression vector, Andrew Mercer for expression of the PanK biosynthetic enzymes, Leanne Barnard for PanK assays, and Andrew Smith for synthesis of CJ-15,801. This project was funded by grants from the National Research Foundation (NRF; FA2007041600013) and Medical Research Council (MRC) of South Africa to E.S., and from National Institutes of Health to V.N. (GM084350), J.C.H. (T32CA009523), and M.D.B. (R01GM086225). R.v.d.W. was supported by a scarce skills scholarship from the NRF. Author contributions: R.v.d.W. prepared the proteins, performed all the PPCS enzyme activity assays and inhibitor characterization studies, and prepared P-CJ-OME; J.C.H. and J.L.M. prepared all other compounds; J.L.M. performed PanK kinetic assays; S.D. and V.N. performed the inhibition studies and analyzed the resulting data; W.J.A.M. performed the melting temperature determinations; S.C.P. was responsible for the modeling studies; M.D.B. and E.S. designed and directed the research, and E.S. wrote the paper with input from all the authors.

Received: December 21, 2011

Revised: March 13, 2012

Accepted: March 27, 2012

Published: May 24, 2012

REFERENCES

- Balibar, C.J., Hollis-Symynkywicz, M.F., and Tao, J. (2011). Pantetheine rescues phosphopantothenoylcysteine synthetase and phosphopantothenoylcysteine decarboxylase deficiency in *Escherichia coli* but not in *Pseudomonas aeruginosa*. *J. Bacteriol.* **193**, 3304–3312.
- Brand, L.A., and Strauss, E. (2005). Characterization of a new pantothenate kinase isoform from *Helicobacter pylori*. *J. Biol. Chem.* **280**, 20185–20188.
- Brownell, J.E., Sintchak, M.D., Gavin, J.M., Liao, H., Bruzzese, F.J., Bump, N.J., Soucy, T.A., Milhollen, M.A., Yang, X., Burkhardt, A.L., et al. (2010). Substrate-assisted inhibition of ubiquitin-like protein-activating enzymes: the NEDD8 E1 inhibitor MLN4924 forms a NEDD8-AMP mimetic in situ. *Mol. Cell* **37**, 102–111.
- Chen, J.J., Tsu, C.A., Gavin, J.M., Milhollen, M.A., Bruzzese, F.J., Mallender, W.D., Sintchak, M.D., Bump, N.J., Yang, X., Ma, J., et al. (2011). Mechanistic studies of substrate-assisted inhibition of ubiquitin-activating enzyme by adenosine sulfamate analogues. *J. Biol. Chem.* **286**, 40867–40877.
- Choudhry, A.E., Mandichak, T.L., Broskey, J.P., Ego, R.W., Kinsland, C., Begley, T.P., Seefeld, M.A., Ku, T.W., Brown, J.R., Zalacain, M., and Ratnam, K. (2003). Inhibitors of pantothenate kinase: novel antibiotics for staphylococcal infections. *Antimicrob. Agents Chemother.* **47**, 2051–2055.
- Cisar, J.S., and Tan, D.S. (2008). Small molecule inhibition of microbial natural product biosynthesis—an emerging antibiotic strategy. *Chem. Soc. Rev.* **37**, 1320–1329.
- Clifton, G., Bryant, S.R., and Skinner, C.G. (1970). N'-(substituted) pantothenamides, antimetabolites of pantothenic acid. *Arch. Biochem. Biophys.* **137**, 523–528.
- Copeland, R.A. (2000). Tight binding inhibitors. In *Enzymes: A Practical Introduction to Structure, Mechanism, and Data Analysis* (New York: Wiley-VCH), pp. 305–317.
- Copeland, R.A. (2005). Tight binding inhibitors. In *Evaluation of Enzyme Inhibitors in Drug Discovery* (Hoboken, NJ: Wiley), pp. 179–213.
- delCardayre, S.B., and Davies, J.E. (1998). *Staphylococcus aureus* coenzyme A disulfide reductase, a new subfamily of pyridine nucleotide-disulfide oxidoreductase. Sequence, expression, and analysis of *cdr*. *J. Biol. Chem.* **273**, 5752–5757.
- Gulick, A.M. (2009). Conformational dynamics in the Acyl-CoA synthetases, adenylation domains of non-ribosomal peptide synthetases, and firefly luciferase. *ACS Chem. Biol.* **4**, 811–827.
- Han, C., Shen, R., Su, S., and Porco, J.A., Jr. (2004). Copper-mediated synthesis of *N*-acyl vinyllogous carbamic acids and derivatives: synthesis of the antibiotic CJ-15,801. *Org. Lett.* **6**, 27–30.
- Hollenhorst, M.A., Ntai, I., Badet, B., Kelleher, N.L., and Walsh, C.T. (2011). A head-to-head comparison of enamide and epoxyamide inhibitors of glucosamine-6-phosphate synthase from the dapdiamide biosynthetic pathway. *Biochemistry* **50**, 3859–3861.
- Hong, B.S., Yun, M.K., Zhang, Y.-M., Chohnan, S., Rock, C.O., White, S.W., Jackowski, S., Park, H.-W., and Leonardi, R. (2006). Prokaryotic type II and type III pantothenate kinases: the same monomer fold creates dimers with distinct catalytic properties. *Structure* **14**, 1251–1261.
- Imtiaz, U., Billings, E., Knox, J.R., Manavathu, E.K., Lerner, S.A., and Mobashery, S. (1993). Inactivation of class A. beta.-lactamases by clavulanic acid: the role of arginine-244 in a proposed nonconcerted sequence of events. *J. Am. Chem. Soc.* **115**, 4435–4442.
- Kim, S., Lee, S.W., Choi, E.C., and Choi, S.Y. (2003). Aminoacyl-tRNA synthetases and their inhibitors as a novel family of antibiotics. *Appl. Microbiol. Biotechnol.* **61**, 278–288.
- Kucharczyk, N., Denisot, M.A., Le Goffic, F., and Badet, B. (1990). Glucosamine-6-phosphate synthase from *Escherichia coli*: determination of the mechanism of inactivation by N3-fumaroyl-L-2,3-diaminopropionic derivatives. *Biochemistry* **29**, 3668–3676.
- Kupke, T. (2002). Molecular characterization of the 4'-phosphopantothenoylcysteine synthetase domain of bacterial dfp flavoproteins. *J. Biol. Chem.* **277**, 36137–36145.
- Kupke, T. (2004). Active-site residues and amino acid specificity of the bacterial 4'-phosphopantothenoylcysteine synthetase CoaB. *Eur. J. Biochem.* **271**, 163–172.
- Lee, J.M., Ahn, D.-S., Jung, D.Y., Lee, J., Do, Y., Kim, S.K., and Chang, S. (2006). Hydrogen-bond-directed highly stereoselective synthesis of Z-enamides via Pd-catalyzed oxidative amidation of conjugated olefins. *J. Am. Chem. Soc.* **128**, 12954–12962.
- Leonardi, R., Chohnan, S., Zhang, Y.-M., Virga, K.G., Lee, R.E., Rock, C.O., and Jackowski, S. (2005). A pantothenate kinase from *Staphylococcus aureus* refractory to feedback regulation by coenzyme A. *J. Biol. Chem.* **280**, 3314–3322.
- Mallett, T.C., Wallen, J.R., Karplus, P.A., Sakai, H., Tsukihara, T., and Claiborne, A. (2006). Structure of coenzyme A-disulfide reductase from *Staphylococcus aureus* at 1.54 Å resolution. *Biochemistry* **45**, 11278–11289.
- Manoj, N., Strauss, E., Begley, T.P., and Ealick, S.E. (2003). Structure of human phosphopantothenoylcysteine synthetase at 2.3 Å resolution. *Structure* **11**, 927–936.
- May, J.J., Finking, R., Wiegshoff, F., Weber, T.T., Bandur, N., Koert, U., and Marahiel, M.A. (2005). Inhibition of the D-alanine:D-alanyl carrier protein ligase from *Bacillus subtilis* increases the bacterium's susceptibility to antibiotics that target the cell wall. *FEBS J.* **272**, 2993–3003.
- Mercer, A.C., and Burkart, M.D. (2007). The ubiquitous carrier protein—a window to metabolite biosynthesis. *Nat. Prod. Rep.* **24**, 750–773.
- Mercer, A.C., Meier, J.L., Torpey, J.W., and Burkart, M.D. (2009). In vivo modification of native carrier protein domains. *ChemBioChem* **10**, 1091–1100.
- Newton, G.L., Arnold, K., Price, M.S., Sherrill, C., Delcardayre, S.B., Aharonowitz, Y., Cohen, G., Davies, J., Fahey, R.C., and Davis, C. (1996). Distribution of thiols in microorganisms: mycothiol is a major thiol in most actinomycetes. *J. Bacteriol.* **178**, 1990–1995.
- Nicely, N.I., Parsonage, D., Paige, C., Newton, G.L., Fahey, R.C., Leonardi, R., Jackowski, S., Mallett, T.C., and Claiborne, A. (2007). Structure of the type III pantothenate kinase from *Bacillus anthracis* at 2.0 Å resolution: implications for coenzyme A-dependent redox biology. *Biochemistry* **46**, 3234–3245.
- Nicolaou, K.C., and Mathison, C.J.N. (2005). Synthesis of imides, *N*-acyl vinyllogous carbamates and ureas, and nitriles by oxidation of amides and amines with Dess-Martin periodinane. *Angew. Chem. Int. Ed. Engl.* **44**, 5992–5997.
- Orhan, G., Bayram, A., Zer, Y., and Balci, I. (2005). Synergy tests by E test and checkerboard methods of antimicrobial combinations against *Brucella melitensis*. *J. Clin. Microbiol.* **43**, 140–143.
- Padayatti, P.S., Helfand, M.S., Totir, M.A., Carey, M.P., Carey, P.R., Bonomo, R.A., and van den Akker, F. (2005). High resolution crystal structures of the trans-enamine intermediates formed by sulbactam and clavulanic acid and E166A SHV-1 β -lactamase. *J. Biol. Chem.* **280**, 34900–34907.
- Padayatti, P.S., Sheri, A., Totir, M.A., Helfand, M.S., Carey, M.P., Anderson, V.E., Carey, P.R., Bethel, C.R., Bonomo, R.A., Buynak, J.D., and van den Akker, F. (2006). Rational design of a β -lactamase inhibitor achieved via stabilization of the trans-enamine intermediate: 1.28 Å crystal structure of wt SHV-1 complex with a penam sulfone. *J. Am. Chem. Soc.* **128**, 13235–13242.
- Patrone, J.D., Yao, J., Scott, N.E., and Dotson, G.D. (2009). Selective inhibitors of bacterial phosphopantothenoylcysteine synthetase. *J. Am. Chem. Soc.* **131**, 16340–16341.
- Pope, A.J., Moore, K.J., McVey, M., Mensah, L., Benson, N., Osbourne, N., Broom, N., Brown, M.J.B., and O'Hanlon, P. (1998). Characterization of isoleucyl-tRNA synthetase from *Staphylococcus aureus*. II. Mechanism of inhibition by reaction intermediate and pseudomonic acid analogues studied using transient and steady-state kinetics. *J. Biol. Chem.* **273**, 31691–31701.
- Saliba, K.J., and Kirk, K. (2005). CJ-15,801, a fungal natural product, inhibits the intraerythrocytic stage of *Plasmodium falciparum* in vitro via an effect on pantothenic acid utilisation. *Mol. Biochem. Parasitol.* **141**, 129–131.

- Schimmel, P., Tao, J., and Hill, J. (1998). Aminoacyl tRNA synthetases as targets for new anti-infectives. *FASEB J.* 12, 1599–1609.
- Sewell, A.L., Villa, M.V.J., Matheson, M., Whittingham, W.G., and Marquez, R. (2011). Fast and flexible synthesis of pantothenic acid and CJ-15,801. *Org. Lett.* 13, 800–803.
- Sieber, S.A., and Marahiel, M.A. (2005). Molecular mechanisms underlying nonribosomal peptide synthesis: approaches to new antibiotics. *Chem. Rev.* 105, 715–738.
- Spry, C., Kirk, K., and Saliba, K.J. (2008). Coenzyme A biosynthesis: an antimicrobial drug target. *FEMS Microbiol. Rev.* 32, 56–106.
- Spry, C., van Schalkwyk, D.A., Strauss, E., and Saliba, K.J. (2010). Pantothenate utilization by *Plasmodium* as a target for antimalarial chemotherapy. *Infect. Disord. Drug Targets* 10, 200–216.
- Stanitzek, S., Augustin, M.A., Huber, R., Kupke, T., and Steinbacher, S. (2004). Structural basis of CTP-dependent peptide bond formation in coenzyme A biosynthesis catalyzed by *Escherichia coli* PPC synthetase. *Structure* 12, 1977–1988.
- Strauss, E. (2010). Coenzyme A biosynthesis and enzymology. In *Comprehensive Natural Products II Chemistry and Biology*, L. Mander and H.-W. Liu, eds. (Oxford: Elsevier), pp. 351–410.
- Strauss, E., and Begley, T.P. (2001). Mechanistic studies on phosphopantothenoylcysteine decarboxylase. *J. Am. Chem. Soc.* 123, 6449–6450.
- Strauss, E., and Begley, T.P. (2002). The antibiotic activity of *N*-pentylpantothenamide results from its conversion to ethyldethia-coenzyme A, a coenzyme A antimetabolite. *J. Biol. Chem.* 277, 48205–48209.
- Strauss, E., Kinsland, C., Ge, Y., McLafferty, F.W., and Begley, T.P. (2001). Phosphopantothenoylcysteine synthetase from *Escherichia coli*. Identification and characterization of the last unidentified coenzyme A biosynthetic enzyme in bacteria. *J. Biol. Chem.* 276, 13513–13516.
- Strauss, E., de Villiers, M., and Rootman, I. (2010). Biocatalytic production of coenzyme A analogues. *ChemCatChem* 2, 929–937.
- Sugie, Y., Dekker, K.A., Hirai, H., Ichiba, T., Ishiguro, M., Shiomi, Y., Sugiura, A., Brennan, L., Duignan, J., Huang, L.H., et al. (2001). CJ-15,801, a novel antibiotic from a fungus, *Seimatosporium* sp. *J. Antibiot.* 54, 1060–1065.
- Thomas, J., and Cronan, J.E. (2010). Antibacterial activity of *N*-pentylpantothenamide is due to inhibition of coenzyme A synthesis. *Antimicrob. Agents Chemother.* 54, 1374–1377.
- van der Westhuyzen, R., and Strauss, E. (2010). Michael acceptor-containing coenzyme A analogues as inhibitors of the atypical coenzyme A disulfide reductase from *Staphylococcus aureus*. *J. Am. Chem. Soc.* 132, 12853–12855.
- van Wyk, M., and Strauss, E. (2008). Development of a method for the parallel synthesis and purification of *N*-substituted pantothenamides, known inhibitors of coenzyme A biosynthesis and utilization. *Org. Biomol. Chem.* 6, 4348–4355.
- Villa, M.V.J., Targett, S.M., Barnes, J.C., Whittingham, W.G., and Marquez, R. (2007). An efficient approach to the stereocontrolled synthesis of enamides. *Org. Lett.* 9, 1631–1633.
- Virga, K.G., Zhang, Y.-M., Leonardi, R., Ivey, R.A., Hevener, K., Park, H.-W., Jackowski, S., Rock, C.O., and Lee, R.E. (2006). Structure-activity relationships and enzyme inhibition of pantothenamide-type pantothenate kinase inhibitors. *Bioorg. Med. Chem.* 14, 1007–1020.
- Wu, G., Robertson, D.H., Brooks, C.L., 3rd, and Vieth, M. (2003). Detailed analysis of grid-based molecular docking: A case study of CDOCKER-A CHARMM-based MD docking algorithm. *J. Comput. Chem.* 24, 1549–1562.
- Yang, K., Eyobo, Y., Brand, L.A., Martynowski, D., Tomchick, D., Strauss, E., and Zhang, H. (2006). Crystal structure of a type III pantothenate kinase: insight into the mechanism of an essential coenzyme A biosynthetic enzyme universally distributed in bacteria. *J. Bacteriol.* 188, 5532–5540.
- Yang, K., Strauss, E., Huerta, C., and Zhang, H. (2008). Structural basis for substrate binding and the catalytic mechanism of type III pantothenate kinase. *Biochemistry* 47, 1369–1380.
- Yao, J., and Dotson, G.D. (2009). Kinetic characterization of human phosphopantothenoylcysteine synthetase. *Biochim. Biophys. Acta* 1794, 1743–1750.
- Yao, J., Patrone, J.D., and Dotson, G.D. (2009). Characterization and kinetics of phosphopantothenoylcysteine synthetase from *Enterococcus faecalis*. *Biochemistry* 48, 2799–2806.
- Zhang, Y.-M., Frank, M.W., Virga, K.G., Lee, R.E., Rock, C.O., and Jackowski, S. (2004). Acyl carrier protein is a cellular target for the antibacterial action of the pantothenamide class of pantothenate antimetabolites. *J. Biol. Chem.* 279, 50969–50975.